The use of molecular graphics and quantum mechanically derived electrostatic potentials to visualize Brönsted acid site strength in zeolites

Patrick J. O'Malley

Department of Chemistry, UMIST, Manchester, UK

The use of the quantum mechanically derived electrostatic potential is introduced to visualize the variation in acidity across a series of cluster molecules corresponding to models of terminal and bridged hydroxyl groups in zeolites. The electrostatic potential is color coded onto the electron density surfaces of the molecules involved, and the variation in acid strength can be followed from the color scheme used. This simple visualization scheme is shown to mirror the experimentally observed acidity variation of terminal hydroxyls, bridged gallium hydroxyls, and bridged aluminium hydroxyls found for zeolites.

From the value of the electrostatic potential near the acidic hydrogen we estimate that the acidity of terminal hydroxyls is similar to acetic acid while the bridged aluminium form is the same as sulphuric acid.

Zeolites are commercially important solid acid catalysts. The acidity of zeolites arises from the presence of hydroxyl groups. In a typical zeolite solid acid, e.g., HZSM-5, two types of hydroxyl groups are present, namely, terminal hydroxyl groups found terminating the crystal lattice or at defect sites and bridged hydroxyl groups found bridging framework silicon and aluminium atoms. A variation in acid strength can be achieved by replacing framework aluminium atoms by gallium.

The use of quantum mechanical calculations to predict the local geometry and intrinsic acidity characteristics of terminal and bridged hydroxyl groups in zeolite frameworks is well known.[1–4] Calculated properties such as the deprotonation energy, the charge distribution in the OH bond, the OH bond length, and the hydroxyl stretching frequency have been shown to be in very good agreement with experimental determinations. In this way, we have a unique probe into the electronic level explanation of acidity in zeolites.

As a measure of intrinsic acidity, all of the above calculated properties have drawbacks. The proton affinity calculation assumes that the ability of the cluster model to accommodate a negative charge is similar to the infinite lattice. This is unlikely to be true, and as such, extrapolating relative acidity values from proton affinity measurements on cluster models to the complete lattice should be treated with caution. Accurate calculation of the deprotonation energy also requires the use of extended basis sets including polarization and diffuse functions, which are prohibitive in terms of cost for larger cluster models. The OH bond length and the hydroxyl stretching frequency are essentially a measure of the difficulty of homolytic fission of the OH bond, and as such, are not a true measure of acidity which corresponds to heterolytic fission. The charge of the hydroxyl hydrogen is thought to be a better representation of acidity, and it can also be directly related to ^{1}H NNR chemical shift determinations.[1] Most studies in this area have used a Mulliken population analysis to determine electrostatic charges. The drawbacks and inconsistencies of this method are well documented,[5,6] and it must be used with caution.

In this study, we introduce the use of the electrostatic potential calculated from the *ab initio* molecular orbital wavefunction as a measure of intrinsic acidity which does not suffer from the drawbacks alluded to above. Also, as most experimental scientists are not readily familiar with quantum chemical terminology, it is important to provide simple and clear exposition of quantum chemical output to aid communication to the nonspecialist. Using molecular graphics techniques, we show how the representation of the electrostatic potential color coded onto the electron density surface of the cluster models employed provides a simple and clear explanation of the variation in acidity observed for terminal hydroxyls, bridged Si/Al hydroxyls, and bridged Si/Ga hydroxyls.

The cluster models used are shown in Figure 1. The *ab initio* molecular orbital calculations were carried out using the SPARTAN program[7] on a Silicon Graphics Indigo

---

workstation. The 3-21G[(*)] basis set was used, and full geometry optimization was performed. No symmetry constraints were imposed. The basis set was chosen because it has been shown to provide molecular geometries and harmonic frequencies equivalent in accuracy to much larger basis sets,[8] and it also allows direct comparison between molecules containing second row and third row elements. Calculation of the second derivative matrix revealed all positive eigenvalues, indicating that all calculated structures corresponded to true minima. The calculated bond lengths and angles for the molecules of Figure 1 are given in Table 1.

Color Plate 1 shows a representation of the electron density calculated at $0.002e/au^3$ for the units of Figure 1. This value of the electron density has been estimated to encompass at least 95% of the electronic charge.[7] The electrostatic potential $V(r)$ that the electrons and nuclei of a molecule create at each point r in the surrounding space is given by the equation

$$V(r) = \sum \frac{Z_A}{|R_A - r|} - \int \frac{\rho(r')\, dr'}{|r' - r|}$$

where Z_A is the charge on nucleus A, located at R_A and $\rho(r)$ is the electronic density function of the molecule. In Color Plate 2 we show a representation of the electrostatic potential computed on the electron density surface described above. The electrostatic potential represents the energy of interaction of a unit positive charge with each point on the electron density surface. Hence positively charged regions of the surface will have positive interaction energies, whereas negative regions will have a negative region of interaction. The coloring scheme represents a gradation in color from blue (representing positive values) through to red (representing negative potentials). The electrostatic potential is represented from the limits of -32.0 kcal/mol to 112.0 kcal/mol. The representation of the electrostatic po-
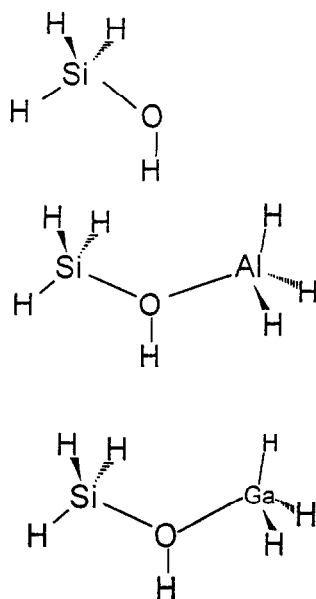

Figure 1. Molecules used to model (a) terminal hydroxyls, (b) bridged aluminium hydroxyls, and (c) bridged gallium hydroxyls.

Table 1. 3-21G(*) calculated bond lengths (Å) and angles (°) for the molecules of Figure 1. While no symmetry constraints were imposed on the calculations, the minimum energy stationary point located exhibited approximate C_s point group symmetry: bond length r and bond angle a

Molecule	H₃SiOH	H₃SiOHAlH₃	H₃SiOHGaH₃
rSiH	1.468	1.471	1.472
rSiH (in plane)	1.478	1.460	1.462
aOSiH	107.3	103.9	105.4
aOSiH (in plane)	112.1	109.1	109.2
aHSiH	107.1	113.0	112.0
aHSiH (in plane)	109.0	110.6	110.3
rSiO	1.633	1.707	1.692
rOH	0.959	0.967	0.966
aSiOH	129.0	120.5	122.4
aSiOAl (SiOGa)		123.8	122.4
rAlO (GaO)		1.940	2.083
rAlH (GaH)		1.610	1.611
rAlH (GaH), in plane		1.605	1.607
aOAlH (OGaH)		95.1	95.2
aOAlH (OGaH), in plane		102.4	99.9
aHAlH (HGaH) aHAlH (HGaH), in plane		116.2 117.5	117.5 118.2

tential color coded onto the electron density map is an excellent method of illustrating the steric (electron density) and electrostatic (color-coded potential) requirements for intermolecular recognition and interaction. Color Plate 2 illustrates the positive region (dark blue) in the vicinity of the hydrogen of the hydroxyl group, a neutral region (green) around the silicon and its hydrogen atoms, and the negatively charged region (red) surrounding the aluminium and gallium hydrogens. The hydroxyl group is clearly associated with the electrophilic region of the molecule. In terms of adsorption at the site, electron-rich regions of the adsorbate

(e.g., the oxygen of alcohols or the π electron system of olefin and aromatics) will present favorable regions for interaction. Hence the darker blue regions can be taken to represent preferred regions for nucleophilic attack by an incoming electron-rich region of a base molecule: the darker the blue color, the greater the interaction of the hydroxyl group hydrogen. The increased interaction should be directly correlated with the inherent capacity of the acid unit to achieve complete transfer of a proton, i.e., the Brönsted acidity. From Color Plate 2 it is clear that the region surrounding the bridged aluminium hydroxyl is more intensely blue colored than the terminal unit; hence based on the preceding arguments, we can predict a greater Brönsted acidity for the bridged aluminium model. From Color Plate 2 it can be seen that the intensity and extent of the blue coloring are less for the Si/Ga (lower left-hand side) hydroxyl than for the Si/Al form (top right-hand side), but are greater than the terminal form (top left-hand side). The intensity and extent of blue covering the hydroxyl group for all three units are seen to vary in the order Al > Ga ≫ terminal. This suggests that the relative attraction for an incoming basic molecule varies in this order as well. This order of acidity is well known from experimental determinations on aluminium and gallium substituted zeolite forms.[9]

The largest positive value of the electrostatic potential is found close to the acidic hydrogen in all cases. In Table 2 we list this value at three values of the electron density (.001 e/au^3, .002 e/au^3, and .004 e/au^3) for the molecules of Figure 1 and also for the two well-known acids, ethanoic acid and sulphuric acid. It is clear from the values on all three electron density surfaces that the terminal hydroxyls have an acidity value close to the weak acid acetic acid whereas the bridged aluminium hydroxyl is estimated to have an acid strength close to sulphuric acid. It is difficult to estimate the strength of acidity in zeolites using indicator methods, but one careful determination of the acidity of acid sites in the large pore HY zeolite indicated an acid strength, of bridged aluminium hydroxyls, similar to 98% sulphuric acid,[10] i.e., in good agreement with our theoretical estimate.

CONCLUSIONS

We have shown that the quantum mechanically derived electrostatic potential represents a good indicator of intrinsic acid site strength for cluster models of acid sites in zeolites. It is a direct measure of the attraction of an acid site for an incoming base molecule. It eliminates the need for charge distribution methods and their associated failings, and provides an easy visual demonstration of acid strength variation. For cluster models of acid sites in zeolites it is particularly useful, as the use of deprotonation energies as an estimate of acid site strength is complicated by the obvious differences in the size of the cluster model and the infinite zeolite lattice. Accurate estimation of deprotonation energies usually requires the use of extended basis sets incor-

Table 2. Maximum value of the electrostatic potential, kcal/mole, calculated on the .001 e/au^3, .002 e/au^3, and .004 e/au^3 electron density surface

Molecule	Electrostatic potential value		
	.001	.002	.004
H_3SiOH	65	84	104
$H_3SiOHAlH_3$	94	112	137
$H_3SiOHGaH_3$	88	106	134
CH_3COOH	60	81	99
H_2SO_4	91	112	136

porating polarization and diffuse functions. Extension to larger models of zeolite acid sites is therefore prohibitively expensive in terms of computational requirements. Relative values of the electrostatic potential would be expected to be accurate even at low basis set level, and hence could be used as a reliable estimate of intrinsic acid site strength for more extended models.

The use of computational chemistry methods is becoming more common in materials science. The information gained from such techniques needs to be conveyed to the nonspecialist in a clear and understandable fashion. In this report we have shown how the molecular graphics representation of the quantum mechanically derived electrostatic potential color coded onto the quantum mechanically derived electron density surface can provide an accurate and easily understandable explanation for the variation in acid site strength across different hydroxyl groups in zeolites.

REFERENCES

1 Sauer, J., *J. Phys. Chem.* 1987, **91**, 2315
2 Sauer, J., *J. Mol. Catal.* 1989, **54**, 312
3 O'Malley, P.J. and Dwyer, J., *Chem. Phys. Lett.* 1988, **143**, 97
4 Nicholas, J.B., Winans, R.E., Harrison, R.J., Iton, L.E., Curtis, L.A., and Hopfinger, A.J., *J. Phys. Chem.* 1992, **96**, 10247
5 Baker, J., *Theoretica Chim. Acta* 1985, **68**, 221
6 Reed, A.E., Weinstock, R.B., and Weinhold, F., *J. Chem. Phys.* 1985, **83**, 735
7 SPARTAN Version 2.0, Wavefunction Inc., Irvine, CA 92715 USA
8 Hehre, W.J., Radom, L., Schleyer, P.v.R., and Pople, J.A., *Ab Initio Molecular Orbital Theory*, Wiley, New York, 1986
9 Chu, C.T.W. and Chang, C.D., *J. Phys. Chem.* 1985, **89**, 1569
10 Kladnig, W.J., *J. Phys. Chem.* 1979, **83**, 765